Winter 12-2016

Combined bulk-rock Hf- and Nd-isotope compositions of Mesoarchaean metavolcanic rocks from the Ivisaartoq Supracrustal Belt, SW Greenland: Deviations from the mantle array caused by crustal recycling

Ali Polat
University of Windsor

Combined bulk-rock Hf- and Nd-isotope compositions of Mesoarchaean metavolcanic rocks from the Ivisaartoq Supracrustal Belt, SW Greenland: Deviations from the mantle array

Kristoffer Szilas[1,*], J. Elis Hoffmann [2,3,4], Toni Schulz [5], Christina Hansmeier [4], Ali Polat [6], Sebastian Viehmann [7], Haino Uwe Kasper [3], Carsten Münker [3]

[1] School of Earth, Energy and Environmental Sciences, Stanford University, California, USA

[2] Institut für Geologische Wissenschaften, Geochemie, Freie Universität Berlin, Berlin, Germany

[3] Institut für Geologie und Mineralogie, Universität zu Köln, Germany

[4] Steinmann Institut, Universität Bonn, Germany

[5] Department of Lithospheric Research, University of Vienna, Austria

[6] Department of Earth and Environmental Sciences, University of Windsor, Ontario, Canada

[7] Jacobs University, Bremen, Germany

* Corresponding author e-mail: szilas@stanford.edu

Abstract

Bulk-rock Lu-Hf and Sm-Nd isotope compositions, as well as major and trace element data are presented for metavolcanic rocks from the Mesoarchaean (ca. 3075 Ma) Ivisaartoq Supracrustal Belt in the Nuuk region of southern West Greenland. The εHf_t calculated at 3075 Ma range from +0.8 to +3.1 and the corresponding εNd_t values range from +0.7 to +3.6, which forms an array that is displaced off the mantle array for these two isotopic systems. Primitive mantle normalized trace element plots of the metabasalts display negative Nb- and Ti-anomalies in combination with the elevated Th abundances, which is consistent with a subduction zone affinity as proposed by previous studies of this metavolcanic belt. No significant correlations are observed between the isotope compositions and proxies of shallow crustal contamination in the Ivisaartoq rocks, despite

clear evidence for inherited Eoarchaean zircon (Polat et al., 2009. Chemical Geology 268, 248-271) which would have dominated the bulk-rock Hf-isotope budget. Furthermore, the measured samples are less radiogenic than the estimate for the depleted mantle composition at 3075 Ma. The lack of isotope and trace element correlation suggests incomplete equilibration between the crustal contaminant and the parental Ivisaartoq melts. We prefer a petrogenetic model with some combination of slab-derived metasomatism of the mantle source region ~~a~~ for the Ivisaartoq magmas, which homogenized their trace element contents, in combination with the incorporation of granitoid restite with unradiogenic Hf-isotope composition at higher degrees of partial melting and finally the eruption of mechanically entrained Eoarchaean crust without significant chemical equilibration. The geochemical arc-affinity and non-DM isotope compositions of these metavolcanic rocks support the notion that crustal recycling and plate tectonics has been operating on Earth since at least the Mesoarchaean Eon.

Keywords: Nuuk region, Godthåbsfjord; Greenstone belt; Metavolcanic rocks; Ujarassuit

1. Introduction

Mesoarchaean supracrustal (greenstone) belts are composed of variably metamorphosed supracrustal lithologies, predominantly mafic to felsic volcanic products, interlayered with gabbros, metaperidotites/serpentinites, and minor amounts of siliciclastic sediments (e.g., Condie, 1981; Eriksson et al., 1994; Condie, 2005). Over the last three decades, detailed geochemical studies of such supracrustal assemblages has documented diverse rock types generated in different tectonic environments, such as arc or plume magmatism in oceanic and continental setting (e.g., Bickle et al., 1983; Puchtel et al., 1993; Polat et al., 1999; Smithies, 2002; Smithies et al., 2004; Kerrich & Polat, 2006).

Because mafic and ultramafic rocks are in most cases mantle-derived, detailed geochemical trace element and isotope studies on these rocks can provide information about the depletion state of the Archaean mantle, which is maintained by the generation of a corresponding continental crustal reservoir (e.g., Sylvester et al., 1997; Polat & Münker, 2004). Moreover, inferences can be made on the composition and depth of the mantle sources, with implications for the geodynamic processes and crust-mantle interaction, such as crustal recycling, source contamination by sediments or contamination processes during the ascent of the magmas (e.g., Chauvel et al., 1985; Appel et al., 2009; Hoffmann et al., 2010).

Measurement of the Sm-Nd isotope compositions of Archaean rocks have revealed high degrees of mantle depletion in the early Earth (e.g., Collerson et al., 1991; Bennett et al., 1993; Bowring and Housh, 1995; Nutman et al., 2007). Bennett et al. (1993) suggested a transitional time period between 3.6 and 2.8 Ga, in which highly depleted reservoirs mixed with enriched components, to homogenize the depleted mantle curve back on a steady-state trend. However, because of the scarcity of Sm-Nd isotope data from highly metamorphosed rocks, it is not possible to distinguish between a "true" mantle depletion signature and post-magmatic disturbance. Therefore, Vervoort & Patchett (1996) applied the more robust Lu-Hf isotope system on early Archaean rocks, because it behaves in tandem with the Sm-Nd isotope system by having a slightly more incompatible radiogenic product than the parental isotope, which thus cause isotopic fractionation of the mantle after melt extraction. These authors did not find a similar signature of a higher depletion-state of the mantle, whereas more recent bulk-rock studies, in which the Lu-Hf isotope system was applied on mafic rocks, do in fact show the presence of such reservoirs in the Archaean Eon (Blichert-Toft & Arndt, 1999; Blichert-Toft et al., 2004; Polat & Münker, 2004; Hoffmann et al., 2010, 2011b). However, it is currently unclear if these reservoirs represent local mantle sources indicative of a specific geodynamic setting (e.g., supra-subduction zones or mantle plumes), or if the early mantle was simply heterogeneous and required further time for homogenization (Hoffmann et al., 2011b).

In this study, we applied the Lu-Hf and Sm-Nd isotope systems in combination with major and trace element analysis on different mafic to ultramafic rocks from the well-characterized Mesoarchaean Ivisaartoq Supracrustal Belt in southern West Greenland (Polat et al., 2007, 2011). The aim of this study is to assess the state of Mesoarchaean mantle depletion and potential mixing signatures resulting from mantle-crust interaction in this region.

2. Geological setting and sampling

The Ivisaartoq-Ujarassuit supracrustal association is situated in the eastern Nuuk region of southern West Greenland (**Fig. 1**), which is part of the North Atlantic craton (Windley and Garde, 2009). In the present work we are solely concerned with the Ivisaartoq Supracrustal Belt, which has been investigated in great detail by several previous studies (Polat et al., 2007, 2008a, 2008b, 2009a, 2009b; Ordóñez-Calderón et al., 2008, 2009). The Ivisaartoq Supracrustal Belt may be correlated with the Qussuk-Bjørneøen Supracrustal Belt (Garde, 2007), located about 50 km to the west (**Fig. 1**), which has a similar age within the analytical error. The region is composed of several 3.9 to ca. 2.8 Ga tectonostratigraphic terranes (e.g., Friend et al., 1988; Nutman et al., 1996; 2004, 2015b; Friend & Nutman, 2005). The continental crust in this region is dominated by orthogneisses of the tonalite-trondhjemite-granodiorite (TTG) suite, which are believed to have formed by partial melting of mafic crust of similar composition as the tholeiitic basalts of the Ivisaartoq Supracrustal Belt (Hoffmann et al., 2011a, 2014; Nagel et al., 2012). The Ivisaartoq Supracrustal Belt represents the largest Mesoarchaean supracrustal belt of southern West Greenland (Appel, 1986, 1994; Polat et al., 2011).

Because of the Mesoarchaean age of the hosting TTG gneisses, the Ivisaartoq Supracrustal Belt is thought to be part of the Kapisilik terrane (Nutman & Friend, 2007). To the west, TTG gneisses of the late Archaean (2830-2800 Ma) Tre Brødre terrane, to the north and northwest TTG gneisses

of the early Archaean (3850-3650 Ma) Isukasia and Færingehavn terranes surround the belt. The supracrustal belt is separated from the surrounding TTGs by late Archaean mylonites (Nutman et al., 1989), and a detailed tectonic interpretation of the structures within the Ivisaartoq sequence is given by Hall & Friend (1983) and Chadwick (1985, 1990).

Detrital zircon from felsic metasediments, which are interlayered with the magmatic components of the belt yielded a U-Pb zircon age of 3075 ±15 Ma (Friend & Nutman, 2005). This age was confirmed by Polat et al. (2008a) with Sm-Nd geochronology on the mafic and ultramafic associations of the belt. A minimum age of 2963 ±12 Ma is defined by crosscutting granitoid intrusions (Friend & Nutman, 2005). The amphibolite units of the Ivisaartoq Supracrustal Belt contain several types of well-preserved primary structures such as: pillow basalts, agglomerates, gabbroic textures, cpx-bearing ultramafic cumulates, volcanic breccias and felsic ocelli (Hall et al., 1987; Polat et al., 2008a, 2008b). An important observation was made by Polat et al. (2009a) who found 3700 Ma inherited zircon grains in pillow lavas from the Ivisaartoq metavolcanic sequence. This evidence of recycled continental crust, in combination with the general depletion of high field strength elements (HFSE) in the volcanic rocks, is strong evidence for a subduction zone setting of the Ivisaartoq Supracrustal Belt (Polat et al., 2011).

The samples used in the present study were collected from low strain domains in the so-called 'upper unit', which were previously described in detail by Polat and co-workers in the above cited studies. The samples selected for the isotope measurements in the present study are fresh and show metamorphic textures as seen in **Figure 2**. They are dominated by hornblende and plagioclase, and oxides generally comprise less than 3 vol.% of the rocks. The major and trace element data and the GPS-positions of the samples can be seen in **Table 1**.

3. Analytical techniques

Rock samples of approximately 2 kg were crushed with a mild steel jaw crusher and powdered using an agate mill. Samples were carefully selected so they did not contain leucosomes, carbonate veins or any obvious signs of post-magmatic alteration. Major element compositions were measured by the XRF method using a Philips PW-1480 spectrometer at Universität Bonn. Trace elements and isotope ratios were measured in powder splits of about 100 mg. These spilts were digested in Parr® bombs using a table top pre-digestion in concentrated HF-HNO_3, followed by 3 days at 180 °C in the bombs and finally digested in $HClO_4$ following the procedures described in Hoffmann et al. (2010). Trace element concentrations were determined by quadrupole ICP–MS, using an Agilent 7500cs at Universität Kiel following the protocol of Garbe-Schönberg (1993). Replicate measurements of the BIR-1 rock standard, as well as of several samples were carried out, which indicated an external reproducibility of <2–4% RSD.

Hafnium and Nd isotope compositions and Lu, Hf, Sm and Nd elemental concentrations were obtained by isotope dilution, employing mixed ^{176}Lu-^{180}Hf and a ^{149}Sm-^{150}Nd spikes and separation by Eichrom® Ln spec resin following the protocols of Münker et al. (2001) and Weyer et al. (2002). From the remaining matrix, Sm and Nd were separated following the method of Pin & Zaldegui (1997). Lutetium, Hf, Sm and Nd were measured using a Finnigan® Neptune MC-ICP-MS at Universität Bonn.

Measured $^{176}Hf/^{177}Hf$ were mass bias corrected to a $^{179}Hf/^{177}Hf$ of 0.7325 using the exponential law. The Münster AMES standard, isotopically indistinguishable from the JMC-475 standard (REF), yielded an average $^{176}Hf/^{177}Hf$ ratio of 0.282160 with an external reproducibility of ±40 ppm (2σ). All of the $^{176}Hf/^{177}Hf$ data are given relative to a JMC-475 value of 0.282160. The typical external reproducibility of the $^{176}Lu/^{177}Hf$ reported in **Table 2** is ±0.2% for ideally spiked samples and also include the effects of error magnification due to non-ideal spike-sample ratios and uncertainties imparted by corrections for Yb interferences (Blichert-Toft et al., 2002; Vervoort et al., 2004; Lagos et al., 2007).

Comment [KS1]: ELIS?

Comment [KS2]: ELIS?

The calculated initial Hf isotope compositions include both the propagated external errors from the measured Hf isotope compositions and the Lu/Hf ratios. For calculation of εHf_t and εNd_t values, a ^{176}Lu decay constant of $1.867x10^{-12}$ (Scherer et al., 2001; Söderlund et al., 2004), a ^{147}Sm decay constant of $6.54x10^{-11}$ (Lugmair & Marti, 1978) and the CHUR values of Bouvier et al. (2008) were used.

All measured $^{143}Nd/^{144}Nd$ data were mass bias corrected using a value of 0.7219 for $^{146}Nd/^{144}Nd$ and the exponential law. During the course of this study the $^{143}Nd/^{144}Nd$ measured for a 20 ppb LaJolla standard solution was 0.511809±20, and all data reported here are given relative to a $^{143}Nd/^{144}Nd$ of 0.511859 for LaJolla. The external reproducibility for $^{143}Nd/^{144}Nd$ measurements was ±30 ppm and ±0.2% for $^{147}Sm/^{144}Nd$. Total procedural blanks during the course of this study were <15 pg for Lu, <57 pg for Hf, and <50 pg for Sm and Nd. All corrections of the isotope compositions to their initial values were made to an age of 3075 Ma, which was demonstrated to be the magmatic age of the Ivisaartoq Supracrustal Belt based on U-Pb zircon dating of a felsic unit by Friend & Nutman (2005).

Comment [KS3]: ELIS?

4. Results

Major and trace element compositions for the Ivisaartoq samples are listed in T**able 1**. The amphibolites (n = 7) are characterized by 49.3–55.7 wt.% SiO_2, 0.52–1.1 wt.% TiO_2, 12.5–15.9 wt.% Al_2O_3, 5.93–12.2 wt.% MgO, 9.10–12.4 wt.% Fe_2O_3 and 10.0–12.5 wt.%. CaO (**Fig. 3**). One of the amphibolites (499332) is slightly more magnesian than the rest of these samples (Fig. 3) and is termed picrite in the rest of this paper. The ultramafic rock (sample 499321) is clearly distinct from the main group of amphibolites by being an amphibole-bearing serpentinite (Figs. 2e and 2f). It has 22.0 wt.% MgO, 5.48 wt.% Al_2O_3, 0.22 wt.% TiO_2 and generally has low abundances of trace element relative to the amphibolites and the serpentinite likely represents a cumulate rock. The trace

element levels are close to the detection limits, which makes this sample susceptible to metasomatic overprinting. We disregard the trace element and isotopic composition of this particular sample in the discussion because of its spiky trace element composition suggests incomplete sample digestion and thus its isotope composition is likely also compromised.

The primitive mantle-normalized trace element patterns of the amphibolites measured in the present study are seen in **Figure 4**. These overlap with those of similar mafic rocks (not shown) from the Ivisaartoq Supracrustal Belt reported by Polat et al. (2007, 2008a, 2008b) and Ordóñez-Calderón (2008, 2009). These trace element patterns show characteristic negative anomalies for Nb and Ti (**Fig. 4**), with the exception of sample 499330, which has positive Nb-anomaly, as well as higher overall levels of incompatible trace element abundances. Sample 499330 also has negative Sr- and Pb-anomalies. Sample 499331 has lower Th concentration than the rest of the samples. Nb/Nb* of the amphibolites range from 0.53 to 1.3, as also expressed by low Nb/Th (2.7–12) and La/Nb (0.95–2.0). Ratios of Zr/Hf of the measured samples are near-chondritic (34–36) and their chondrite-normalized rare earth element (REE) patterns have La_{CN}/Yb_{CN} ratios of 0.84 to 1.3 and La_{CN}/Sm_{CN} ratios of 0.73 to 1.3.

The bulk-rock Lu-Hf and Sm-Nd isotope data for the measured samples from the Ivisaartoq Supracrustal Belt are presented in **Table 2**. Ratios of $^{176}Lu/^{177}Hf$ measured in the Ivisaartoq rocks range from 0.02673 to 0.03346 and $^{147}Sm/^{144}Nd$ in the same sample splits are between 0.1872 and 0.2073. The εHf_t calculated to 3075 Ma range from +0.8 to +3.1 (**Fig. 6**). The ultramafic sample (499321) yields a significantly more radiogenic εHf_t composition of +7.5. However, as mentioned above we disregard the ultramafic sample in the discussion of the isotope data based on its low Hf concentration, which would make this particular sample prone to metasomatic overprinting. Additionally, there could have been an issue with the sample digestion, which is indicated by the saw-tooth trace element pattern of this sample (not shown) with negative Zr-Ti-Y-Lu-anomalies. εNd_t values of the measured mafic rocks and the picrite from Ivisaartoq range from +0.7 to +3.6.

None of the two isotope systems yield true isochrons, which is to be expected due to the relatively wide range of initial ε-values for the Ivisaartoq amphibolites. This indicates that these rocks have either experienced crustal contamination or that their mantle source region was heterogeneous or variably overprinted by a crustal component.

5. Discussion

Previous studies have documented that at an early stage hydrothermal seafloor alteration affected Archaean supracrustal rocks in the Nuuk region (e.g., Polat & Hofmann, 2003; Szilas & Garde, 2013). Ordóñez-Calderón et al. (2008) discussed the different types of alteration found within the Ivisaartoq Supracrustal Belt, and as mentioned in **Section 2**, in this work we specifically selected samples which did not display any petrographic evidence of alteration. In addition the calculated W-index of Ohta & Arai (2007) for all Ivisaartoq samples used in this work is less than 6.6, which supports the inference that they have not experienced hydrothermal alteration. Furthermore these samples plot within the geochemical range of previous results from this metavolcanic sequence (**Fig. 3**). Hence alteration is regarded as unlikely to have significantly affected the materials discussion in detail below.

Although we present a relatively small geochemical data set, it is obvious from **Figure 3** that our data shows similar geochemical trend as existing data from the Ivisaartoq Supracrustal Belt. The combined data sets outline geochemical trends that are consistent with fractional crystallization processes. The ultramafic rocks (serpentinites) from the Ivisaartoq Supracrustal Belt are similar in composition to serpentinites and amphibolite-phlogopite schists found in other Archaean supracrustal sequences of southern West Greenland (e.g., Szilas et al., 2012b, 2014a, 2015b). Such ultramafic rocks typically represent olivine±pyroxene cumulates, which can be related directly to the associated metavolcanic rocks through fractional crystallization of a primitive melt.

Significant crustal assimilation during fractional crystallisation processes (AFC) is not supported due to the relatively high Mg, Cr and Ni contents of the metavolcanic rocks and the general lack of correlation with their isotope compositions (Figures 3 and 8). We note that all of the measured samples from the Ivisaartoq Supracrustal Belt plot within the region of subduction-related rocks in a Th/Yb vs. Nb/Yb binary tectonic discrimination diagram (**Fig. 5**), similar to the vast majority of Mesoarchaean mafic-andesitic supracrustal rocks from southern West Greenland (e.g., Szilas et al., 2011, 2013a, 2013b, 2014b). However, as shown recently by Li et al. (2015), such tectonic discrimination plots do not adequately capture the geochemical differences of contrasting geological settings. Nevertheless, this plot is useful as a reference for comparison with the existing data from the Ivisaartoq Supracrustal Belt. The primitive mantle (PM) normalized diagrams (as shown in **Figure 4**) further aid in distinguishing between different volcanic environments and their mantle sources. The distinctly negative Nb- and Ti-anomalies that are seen in all of our Ivisaartoq samples (except for sample 499330), in combination with the elevated Th contents is most easily explained as a feature imparted through subduction zone processes, where the mantle wedge was influenced by a slab-derived component. This finding is consistent with previous studies of the Ivisaartoq Supracrustal Belt who indicated subduction derived geochemical signatures (Polat et al., 2007; Ordóñez-Calderón et al., 2008). The positive Pb-anomalies likely reflect a crustal metasomatic input during subduction zone processes or alternatively may emanate from an early stage of seafloor alteration of the basaltic sequence. The positive Sr-anomalies however are more ambiguous, as they could either represent a metasomatic addition during metamorphism, or more likely they may be primary and reflect accumulation of plagioclase in the magmas.

Polat et al. (2009a) documented evidence for crustal contamination of the metavolcanic rocks from the Ivisaartoq Supracrustal Belt in the form of preserved Eoarchaean zircon within ocelli (felsic inclusions) in pillow basalts, which were likely derived from the adjacent Itsaq Gneiss Complex (**Fig. 1**). As shown by Bennett and Nutman (2014) and Nutman et al. (2015a, 2016), such

Eoarchaean felsic crust would have had a near-chondritic initial isotope composition. This crust would then have evolved to an isotope composition with εHf_t of around -15.8 by 3075 Ma, at the time of eruption of the Ivisaartoq volcanic sequence (**Fig. 6**). Thus, there appears to have been a distinct contribution from an unradiogenic component (similar to Isua TTGs) in the mantle source of the Ivisaartoq rocks in terms of their Hf- and Nd-isotope compositions. This may in turn account for the negative Nb- and Ti-anomalies that are observed in **Figure 4**, as well as the lack of correlation between trace elements and isotope compositions. This would also explain why our data do not yield any consistent isochrons as their apparent initial ε-values scatter significantly.

Figure 7 shows a plot of εHf_t vs. εNd_t for the Ivisaartoq amphibolites. Most of these samples deviate from the mantle array, such decoupling between the Hf and Nd systems is typically explained by the presence of garnet in the source region during partial melting, which retains HREE in the restite (Hoffmann et al., 2011b). However, such a model in this instance is not supported given that the picrite sample, which supposedly represents the highest degree of melting among these samples, also has a flat HREE-pattern similar to that of the other amphibolite samples (**Fig. 4**). If garnet was involved in the picrite genesis this sample's HREE patterns would be expected to have fractionated from its LREE pattern.

εNd_t and εHf_t display an apparent inverse correlation with La/Sm and Th/Nb, whereas they are overall positively correlated with Nb/Nb* (**Fig. 8**). This would at first appear to support crustal contamination involving an evolved incompatible trace element-rich assimilant with negative HFSE-anomalies and unradiogenic isotope compositions. However, these trends are mainly controlled by samples 499330 and 499331, which from **Figure 4** can be seen to both be anomalous by having a positive Nb- and negative Th anomaly, respectively. The elevated Nb of sample 499330 cannot be accounted for by dilution with a crustal assimilant, which would have even lower Nb content and such a source would also likely have low HREE concentration relative to the metabasalts. This sample has likely accumulated a Nb-rich phase, because it is not unusual in any

277 other regard in comparison to the rest of the Ivisaartoq samples. The elevated Th of samples 499331
278 in combination with its relatively unradiogenic isotope compositions is also not consistent with a
279 crustal assimilant. Excluding these two anomalous samples, there is no obvious correlation between
280 the contamination-sensitive trace elements and the isotope compositions. In fact all of the samples
281 would essentially have similar trace element ratios.

282 The picritic sample (499332) with a MgO content of 12.2 wt.%, has the most radiogenic Nd-
283 isotope composition, but the least radiogenic Hf-isotope composition (**Fig. 7**). Given that there are
284 technically no correlations between the isotope compositions and the major or trace elemental
285 abundances of the measured samples as mentioned above, the observed range of the Hf- and Nd-
286 isotope data seem to reflect a variable mantle source composition, rather than crustal assimilation
287 during the eruption of the volcanic rocks. Alternatively, any crustal assimilant would have had to be
288 introduced into the mantle source region of the volcanic rocks from the Ivisaartoq Supracrustal Belt.
289 The apparent decoupling of the Hf- and Nd-isotope systematics that is seen in **Figure 7** is typical of
290 Archaean TTGs (Hoffmann et al., 2011b); however, as seen in Figure 4, all of the measured
291 Ivisaartoq samples have similar HREE-patterns. Thus, garnet fractionation in either the mantle
292 source or within a deep magma chamber of the Ivisaartoq rocks cannot explain their isotopic
293 variation. One possible way of imparting an unradiogenic Hf-isotope signature on a magma derived
294 from an otherwise depleted mantle source could be to have a residual HFSE-rich phase that is only
295 fused at higher degrees of partial melting. This could potentially explain why the picritic sample,
296 which likely experienced the highest degree of melting, has the largest deviation from the mantle
297 array and yet appears to have sampled the most depleted part of the mantle source in terms of the
298 Nd-isotope composition (**Fig. 7**). This also means that at lower degrees of partial melting, the
299 Ivisaartoq magma would sample a higher proportion of any fusible component such as pyroxenite
300 or slab-derived contributions in the mantle source region. This explanation is consistent with the
301 observed wide range in isotope values without any significant trace element variation.

Another possible way to explain these observations is that the mantle source of the Ivisaartoq rocks was overprinted by a slab melt component and/or by mélange diapirs (c.f., Marschall & Schumacher, 2012) in a subduction zone. In this way Eoarchaean sediments could have been recycled back into the mantle source region carrying with them the zircon-bearing crustal material that imparted subduction zone characteristics of the Ivisaartoq metavolcanic rocks. Zircon would potentially only have been fused during higher melting degrees, which could explain why the picritic sample is the most decoupled. However, the latter model is difficult to reconcile with the apparent lack of thermal equilibration of felsic zircon-bearing material, which would likely require hybridisation of low temperature serpentine-dominated sediment diapirs and mantle-derived melts. Alternatively, the domains in the metavolcanic rocks that host Eoarchaean zircon may represent entrainment of pre-existing crust during eruption without significant equilibration with the hosting arc-related magmas, but in this case a subduction zone component would still be needed in the source region of the Ivisaartoq magmas in order to explain their trace element patterns in combination with their relatively high Mg, Cr and Ni contents. In our opinion a model where HFSE-rich ilmenite/rutile derived as a restite by TTG-formation that was present in the mantle source of the Ivisaartoq metavolcanic rocks, is plausible. If this component was only contributing to the melt at high degrees of melting, such as those experiences by the picritic rock then this sample could inherited an unusually unradiogenic Hf-isotope composition, despite sampling more of the depleted mantle domain as seen by its Nd-isotope composition (**Fig. 7**).Overall the trace element and isotope compositions of the metavolcanic rocks from the Ivisaartoq supracrustal belt are consistent with some degree of crustal recycling during the Mesoarchaean. In addition our results are compatible with a subduction zone-related origin for at least some components of the supracrustal belts in southern West Greenland (e.g., Windley & Garde, 2009; Polat et al., 2011, 2015).

6. Conclusions

Based on new $^{176}Lu/^{176}Hf$ and $^{147}Sm/^{143}Nd$ isotope data, as well as major and trace element data for volcanic rocks from the Mesoarchaean Ivisaartoq Supracrustal Belt, the following is apparent:

- The Lu-Hf and Sm-Nd isotope systematics of the measured amphibolites from the Ivisaartoq Supracrustal Belt define an array that deviates from the mantle array and broadly overlaps with TTGs from this region.

- The metavolcanic rocks are not juvenile and have Hf- and Nd-isotope compositions distinctly less radiogenic than predicted depleted mantle at the time of eruption.

- Negative Nb- and Ti-anomalies in combination with elevated Th abundances for the amphibolites is consistent with a subduction zone affinity.

- No clear correlation exists between initial Hf- and Nd-isotope compositions and proxies for shallow crustal contamination (AFC processes).

Given the above two distinct petrogenetic models can be proposed for the Ivisaartoq metavolcanic rocks:

(1) The lack of AFC-processes recorded in these rocks demonstrates that crustal contamination did not occur during the eruption of these magmas through pre-existing continental crust. Instead, we suggest that the mantle source region of the Ivisaartoq magmas contained remnants of TTG-derived restite with an unradiogenic component which fused into the magma at higher degrees of partial melting, such as those possibly attained by the picritic rock.

(2) Alternatively, Eoarchaean sediments could have been recycled back into the mantle source region carrying with them zircon-bearing crustal material that imparted the subduction zone characteristics to the Ivisaartoq metavolcanic rocks. In this scenario zircon would also only have been fused during higher melting degrees, consistent with the picritic sample's decoupled Nd- and Hf-isotopic signature.

Currently the presented data set does not permit unequal distinction between these two scenarios. However, it does point out an intriguing decoupled Lu-Hf and Sm-Nd signature which may have significance for processes related to Archaean metavolcanic rocks and their geodynamic settings.

Acknowledgements

We thank R. Hoffbauer for help with the XRF-analysis. Dieter Garbe-Schönberg and his team are acknowledged for quadrupole ICP-MS analyses in Kiel and Cologne. The Geological Survey of Denmark and Greenland (GEUS) is thanked for permission to publish this work. We greatly appreciate the editorial handling and review comments by Dewashish Upadhyay, and acknowledge the constructive critique by an anonymous reviewer, which significantly improved the manuscript. Discussions with Christopher Kirkland were also highly valued as they contributed positively to this study.

References

Appel, P. U. (1986). Strata bound scheelite in the Archean Malene supracrustal belt, West Greenland. Mineralium Deposita, 21(3), 207-215.

Appel, P. U. (1994). Stratabound scheelite in altered Archaean komatiites, West Greenland. Mineralium Deposita, 29(4), 341-352.

Appel, P. W., Polat, A., & Frei, R. (2009). Dacitic ocelli in mafic lavas, 3.8–3.7 Ga Isua greenstone belt, West Greenland: geochemical evidence for partial melting of oceanic crust and magma mixing. Chemical Geology, 258(3), 105-124.

Bennett, V. C., Nutman, A. P., & McCulloch, M. T. (1993). Nd isotopic evidence for transient, highly depleted mantle reservoirs in the early history of the Earth. Earth and Planetary Science Letters, 119(3), 299-317.

Bennett, V. & Nutman, A.P. (2014). Geologically Controlled Isotope-Time Patterns Reveal Early Differentiation and Crust Formation Processes. AGU Fall Meeting Abstracts. Vol. 1.

Bickle, M. J., Bettenay, L. F., Barley, M. E., Chapman, H. J., Groves, D. I., Campbell, I. H., & De Laeter, J. R. (1983). A 3500 Ma plutonic and volcanic calc-alkaline province in the Archaean East Pilbara Block. Contributions to Mineralogy and Petrology, 84(1), 25-35.

Blichert-Toft, J., & Arndt, N. T. (1999). Hf isotope compositions of komatiites. Earth and Planetary Science Letters, 171(3), 439-451.

Blichert-Toft, J., Boyet, M., Télouk, P., & Albarède, F. (2002). 147 Sm–143 Nd and 176 Lu–176 Hf in eucrites and the differentiation of the HED parent body. Earth and Planetary Science Letters, 204(1), 167-181.

Blichert-Toft, J., Arndt, N. T., & Gruau, G. (2004). Hf isotopic measurements on Barberton komatiites: effects of incomplete sample dissolution and importance for primary and secondary magmatic signatures. Chemical Geology, 207(3), 261-275.

Bouvier, A., Vervoort, J. D., & Patchett, P. J. (2008). The Lu–Hf and Sm–Nd isotopic composition of CHUR: constraints from unequilibrated chondrites and implications for the bulk composition of terrestrial planets. Earth and Planetary Science Letters, 273(1), 48-57.

Bowring, S.A., & Housh, T., (1995). The Earth's early evolution. Science 269, 1535-1540.

Chadwick, B. (1985). Contrasting styles of tectonism and magmatism in the late Archaean crustal evolution of the northeastern part of the Ivisârtoq region, inner Godthåbsfjord, southern West Greenland. Precambrian research, 27(1), 215-238.

Chadwick, B. (1990). The stratigraphy of a sheet of supracrustal rocks within high-grade orthogneisses and its bearing on Late Archaean structure in southern West Greenland. Journal of the Geological Society, 147(4), 639-652.

Chauvel, C., Dupré, B., & Jenner, G. A. (1985). The Sm-Nd age of Kambalda volcanics is 500 Ma too old!. Earth and Planetary Science Letters, 74(4), 315-324.

Collerson, K. D., Campbell, L. M., Weaver, B. L., & Palacz, Z. A. (1991). Evidence for extreme mantle fractionation in early Archaean ultramafic rocks from northern Labrador.

Condie, K. C. (1981). Archean greenstone belts. Elsevier, Amsterdam, 433 pp. ISBN: 978-0-444-41854-8.

Condie, K. C. (2005). High field strength element ratios in Archean basalts: a window to evolving sources of mantle plumes?. Lithos, 79(3), 491-504.

Eriksson, K. A., Krapez, B., & Fralick, P. W. (1994). Sedimentology of Archean greenstone belts: signatures of tectonic evolution. Earth-Science Reviews, 37(1), 1-88.

Friend, C. R., & Nutman, A. P. (2005). New pieces to the Archaean terrane jigsaw puzzle in the Nuuk region, southern West Greenland: steps in transforming a simple insight into a complex regional tectonothermal model. Journal of the Geological Society, 162(1), 147-162.

Friend, C. R. L., Nutman, A. P., & McGregor, V. R. (1988). Late Archaean terrane accretion in the Godthåb region, southern West Greenland. Nature, 335, 535-538.

Gale, A., Dalton, C.A., Langmuir, C.H., Su, Y. & Schilling, J.G. (2013). The mean composition of ocean ridge basalts. Geochemistry, Geophysics, Geosystems 14, 489-518.

Garbe-Schönberg, C.D. (1993). Simultaneous Determination of Thirty-Seven Trace Elements in Twenty-Eight International Rock Standards By ICP-MS. Geostandards Newsletter 17, 81-97.

452 Garde, A. A. (2007). A mid-Archaean island arc complex in the eastern Akia terrane,
453 Godthåbsfjord, southern West Greenland. Journal of the Geological Society, 164(3), 565-579.
454
455 Hall, R. P., & Friend, C. R. L. (1983). Intrusive relationships between young and old Archaean
456 gneisses: evidence from Ivisărtoq, southern West Greenland. Geological Journal, 18(1), 77-91.
457
458 Hall, R. P., Hughes, D. J., & Friend, C. R. L. (1987). Mid-Archaean basic magmatism of southern
459 West Greenland. Geological Society, London, Special Publications, 27(1), 261-275.
460
461 Hoffmann, J. E., Münker, C., Polat, A., König, S., Mezger, K., & Rosing, M. T. (2010). Highly
462 depleted Hadean mantle reservoirs in the sources of early Archean arc-like rocks, Isua supracrustal
463 belt, southern West Greenland. Geochimica et Cosmochimica Acta, 74(24), 7236-7260.
464
465 Hoffmann, J. E., Münker, C., Næraa, T., Rosing, M. T., Herwartz, D., Garbe-Schönberg, D., &
466 Svahnberg, H. (2011a). Mechanisms of Archean crust formation inferred from high-precision HFSE
467 systematics in TTGs. Geochimica et Cosmochimica Acta, 75(15), 4157-4178.
468
469 Hoffmann, J. E., Münker, C., Polat, A., Rosing, M. T., & Schulz, T. (2011b). The origin of
470 decoupled Hf–Nd isotope compositions in Eoarchean rocks from southern West Greenland.
471 Geochimica et Cosmochimica Acta, 75(21), 6610-6628.
472
473 Hoffmann, J. E., Svahnberg, H., Piazolo, S., Scherstén, A., & Münker, C. (2012). The geodynamic
474 evolution of Mesoarchean anorthosite complexes inferred from the Naajat Kuuat Complex, southern
475 West Greenland. Precambrian Research, 196, 149-170.
476

Hoffmann, J. E., Nagel, T. J., Münker, C., Næraa, T., & Rosing, M. T. (2014). Constraining the process of Eoarchean TTG formation in the Itsaq Gneiss Complex, southern West Greenland. Earth and Planetary Science Letters, 388, 374-386.

Kerrich, R., & Polat, A. (2006). Archean greenstone-tonalite duality: Thermochemical mantle convection models or plate tectonics in the early Earth global dynamics?. Tectonophysics, 415(1), 141-165.

Lagos, M., Scherer, E. E., Tomaschek, F., Münker, C., Keiter, M., Berndt, J., & Ballhaus, C. (2007). High precision Lu–Hf geochronology of Eocene eclogite-facies rocks from Syros, Cyclades, Greece. Chemical Geology, 243(1), 16-35.

Li, C., Arndt, N. T., Tang, Q., & Ripley, E. M. (2015). Trace element indiscrimination diagrams. Lithos, 232, 76-83.

Lugmair, G. W., & Marti, K. (1978). Lunar initial 143 Nd/144 Nd: differential evolution of the lunar crust and mantle. Earth and Planetary Science Letters, 39(3), 349-357.

Marschall, H. R., & Schumacher, J. C. (2012). Arc magmas sourced from mélange diapirs in subduction zones. Nature Geoscience, 5(12), 862-867.

Münker, C., Weyer, S., Scherer, E., & Mezger, K. (2001). Separation of high field strength elements (Nb, Ta, Zr, Hf) and Lu from rock samples for MC-ICPMS measurements. Geochemistry, Geophysics, Geosystems, 2(12).

Nagel, T. J., Hoffmann, J. E., & Münker, C. (2012). Generation of Eoarchean tonalite-trondhjemite-granodiorite series from thickened mafic arc crust. Geology, 40(4), 375-378.

Nutman, A. P., & Friend, C. R. (2007). Adjacent terranes with ca. 2715 and 2650Ma high-pressure metamorphic assemblages in the Nuuk region of the North Atlantic Craton, southern West Greenland: Complexities of Neoarchaean collisional orogeny. Precambrian Research, 155(3), 159-203.

Nutman, A. P., Friend, C. R., Baadsgaard, H., & McGregor, V. R. (1989). Evolution and assembly of Archean gneiss terranes in the Godthåbsfjord region, southern West Greenland: structural, metamorphic, and isotopic evidence. Tectonics, 8(3), 573-589.

Nutman, A. P., McGregor, V. R., Friend, C. R., Bennett, V. C., & Kinny, P. D. (1996). The Itsaq Gneiss Complex of southern West Greenland; the world's most extensive record of early crustal evolution (3900-3600 Ma). Precambrian Research, 78(1), 1-39.

Nutman, A. P., Friend, C. R., Barker, S. L., & McGregor, V. R. (2004). Inventory and assessment of Palaeoarchaean gneiss terrains and detrital zircons in southern West Greenland. Precambrian Research, 135(4), 281-314.

Nutman, A. P., Bennett, V. C., Friend, C. R., Horie, K., & Hidaka, H. (2007). ~ 3,850 Ma tonalites in the Nuuk region, Greenland: geochemistry and their reworking within an Eoarchaean gneiss complex. Contributions to Mineralogy and Petrology, 154(4), 385-408.

526 Nutman, A. P., Bennett, V. C., & Friend, C. R. (2015a). Proposal for a continent
527 'Itsaqia'amalgamated at 3.66 Ga and rifted apart from 3.53 Ga: Initiation of a Wilson Cycle near the
528 start of the rock record. American Journal of Science, 315(6), 509-536.
529
530 Nutman, A. P., Bennett, V. C., & Friend, C. R. (2015b). The emergence of the Eoarchaean proto-
531 arc: evolution of a c. 3700 Ma convergent plate boundary at Isua, southern West Greenland.
532 Geological Society, London, Special Publications, 389(1), 113-133.
533
534 Nutman, A. P., Bennett, V. C., Friend, C. R., Yi, K., & Lee, S. R. (2015c). Mesoarchaean collision
535 of Kapisilik terrane 3070Ma juvenile arc rocks and> 3600Ma Isukasia terrane continental crust
536 (Greenland). Precambrian Research, 258, 146-160.
537
538 Ohta, T., & Arai, H. (2007). Stastical empirical index of chemical weathering in igneous rocks: a
539 new tool for evaluating the degree of weathering. Chemical Geology 240, 280-297.
540
541 Ordóñez-Calderón, J. C., Polat, A., Fryer, B. J., Gagnon, J. E., Raith, J. G., & Appel, P. W. U.
542 (2008). Evidence for HFSE and REE mobility during calc-silicate metasomatism, Mesoarchean (~
543 3075Ma) Ivisaartoq greenstone belt, southern West Greenland. Precambrian Research, 161(3), 317-
544 340.
545
546 Ordóñez-Calderón, J. C., Polat, A., Fryer, B. J., Appel, P. W. U., van Gool, J. A. M., Dilek, Y., &
547 Gagnon, J. E. (2009). Geochemistry and geodynamic origin of the Mesoarchean Ujarassuit and
548 Ivisaartoq greenstone belts, SW Greenland. Lithos, 113(1), 133-157.
549

Pin, C., & Zalduegui, J. S. (1997). Sequential separation of light rare-earth elements, thorium and uranium by miniaturized extraction chromatography: application to isotopic analyses of silicate rocks. Analytica Chimica Acta, 339(1), 79-89.

Polat, A., & Hofmann, A. W. (2003). Alteration and geochemical patterns in the 3.7–3.8 Ga Isua greenstone belt, West Greenland. Precambrian Research, 126(3), 197-218.

Polat, A., & Münker, C. (2004). Hf–Nd isotope evidence for contemporaneous subduction processes in the source of late Archean arc lavas from the Superior Province, Canada. Chemical Geology, 213(4), 403-429.

Polat, A., Kerrich, R., & Wyman, D. A. (1999). Geochemical diversity in oceanic komatiites and basalts from the late Archean Wawa greenstone belts, Superior Province, Canada: trace element and Nd isotope evidence for a heterogeneous mantle. Precambrian Research, 94(3), 139-173.

Polat, A., Appel, P. W., Frei, R., Pan, Y., Dilek, Y., Ordóñez-Calderón, J. C., & Raith, J. G. (2007). Field and geochemical characteristics of the Mesoarchean (~ 3075Ma) Ivisaartoq greenstone belt, southern West Greenland: Evidence for seafloor hydrothermal alteration in supra-subduction oceanic crust. Gondwana Research, 11(1), 69-91.

Polat, A., Frei, R., Appel, P. W. U., Dilek, Y., Fryer, B., Ordóñez-Calderón, J. C., & Yang, Z. (2008a). The origin and compositions of Mesoarchean oceanic crust: evidence from the 3075 Ma Ivisaartoq greenstone belt, SW Greenland. Lithos, 100(1), 293-321.

575 Polat, A., Frei, R., Appel, P. W., Fryer, B., Dilek, Y., & Ordóñez-Calderón, J. C. (2008b). An
576 overview of the lithological and geochemical characteristics of the Mesoarchean (ca. 3075 Ma)
577 Ivisaartoq greenstone belt, southern West Greenland. Geological Society of America Special
578 Papers, 440, 51-76.
579
580 Polat, A., Frei, R., Fryer, B., & Appel, P. W. (2009a). The origin of geochemical trends and
581 Eoarchean (ca. 3700Ma) zircons in Mesoarchean (ca. 3075Ma) ocelli-hosting pillow basalts,
582 Ivisaartoq greenstone belt, SW Greenland: Evidence for crustal contamination versus crustal
583 recycling. Chemical Geology, 268(3), 248-271.
584
585 Polat, A., Kerrich, R., & Windley, B. (2009b). Archaean crustal growth processes in southern West
586 Greenland and the southern Superior Province: geodynamic and magmatic constraints. Geological
587 Society, London, Special Publications, 318(1), 155-191.
588
589 Polat, A., Appel, P. W., & Fryer, B. J. (2011). An overview of the geochemistry of Eoarchean to
590 Mesoarchean ultramafic to mafic volcanic rocks, SW Greenland: implications for mantle depletion
591 and petrogenetic processes at subduction zones in the early Earth. Gondwana Research, 20(2), 255-
592 283.
593
594 Polat, A., Wang, L., & Appel, P. W. (2015). A review of structural patterns and melting processes
595 in the Archean craton of West Greenland: Evidence for crustal growth at convergent plate margins
596 as opposed to non-uniformitarian models. Tectonophysics 662, 67-94 .
597

598 Puchtel, I. S., Zhuravlev, D. Z., Samsonov, A. V., & Arndt, N. T. (1993). Petrology and
599 geochemistry of metamorphosed komatiites and basalts from the Tungurcha greenstone belt, Aldan
600 Shield. Precambrian Research, 62(4), 399-417.
601
602 Sarbas, B., & Nohl, U. (2008). The GEOROC database as part of a growing geoinformatics
603 network. In: Brady, S.R., Sinha, A.K., and Gundersen, L.C. (Eds), Geoinformatics 2008 - Data to
604 Knowledge, U.S. Geological Survey Scientific Investigations Report, Proceedings, 42-43.
605
606 Scherer, E., Münker, C., & Mezger, K. (2001). Calibration of the lutetium-hafnium clock. Science,
607 293(5530), 683-687.
608
609 Smithies, R. H. (2002). Archaean boninite-like rocks in an intracratonic setting. Earth and Planetary
610 Science Letters, 197(1), 19-34.
611
612 Smithies, R. H., Champion, D. C., & Sun, S. S. (2004). The case for Archaean boninites.
613 Contributions to Mineralogy and Petrology, 147(6), 705-721.
614
615 Söderlund, U., Patchett, P. J., Vervoort, J. D., & Isachsen, C. E. (2004). The 176 Lu decay constant
616 determined by Lu–Hf and U–Pb isotope systematics of Precambrian mafic intrusions. Earth and
617 Planetary Science Letters, 219(3), 311-324.
618
619 Sylvester, I.H. Campbell, & D.A. Bowyer, (1997). Niobium/Uranium evidence for early formation
620 of the continental crust, Science 275, 521-523.
621

622 Szilas, K., & Garde, A. A. (2013). Mesoarchaean aluminous rocks at Storø, southern West
623 Greenland: new age data and evidence of premetamorphic seafloor weathering of basalts. Chemical
624 Geology, 354, 124-138.
625
626 Szilas, K., Van Hinsberg, V. J., Kisters, A. F., Kokfelt, T. F., Scherstén, A., & Windley, B. F.
627 (2011). Remnants of Mesoarchaean oceanic crust in the Tartoq Group, South-West Greenland.
628 Geological Survey of Denmark and Greenland Bulletin, 23, 57-60.
629
630 Szilas, K., Hoffmann, J. E., Scherstén, A., Rosing, M. T., Windley, B. F., Kokfelt, T. F., & Münker,
631 C. (2012a). Complex calc-alkaline volcanism recorded in Mesoarchaean supracrustal belts north of
632 Frederikshåb Isblink, southern West Greenland: Implications for subduction zone processes in the
633 early Earth. Precambrian Research, 208, 90-123.
634
635 Szilas, K., Næraa, T., Scherstén, A., Stendal, H., Frei, R., van Hinsberg, V. J., & Rosing, M. T.
636 (2012b). Origin of Mesoarchaean arc-related rocks with boninite/komatiite affinities from southern
637 West Greenland. Lithos, 144, 24-39.
638
639 Szilas, K., Hoffmann, J. E., Scherstén, A., Kokfelt, T. F., & Münker, C. (2013a). Archaean andesite
640 petrogenesis: insights from the Grædefjord Supracrustal Belt, southern West Greenland.
641 Precambrian Research, 236, 1-15.
642
643 Szilas, K., Van Hinsberg, V. J., Kisters, A. F., Hoffmann, J. E., Windley, B. F., Kokfelt, T. F., &
644 Münker, C. (2013b). Remnants of arc-related Mesoarchaean oceanic crust in the Tartoq Group of
645 SW Greenland. Gondwana Research, 23(2), 436-451.
646

647 Szilas, K., Van Hinsberg, V. J., Creaser, R. A., & Kisters, A. F. (2014a). The geochemical
648 composition of serpentinites in the Mesoarchaean Tartoq Group, SW Greenland: Harzburgitic
649 cumulates or melt-modified mantle?. Lithos, 198, 103-116.
650
651 Szilas, K., Hoffmann, J. E., Münker, C., Dziggel, A., & Rosing, M. T. (2014b). Eoarchean within-
652 plate basalts from southwest Greenland: Comment. Geology, 42(3), e330-e330.
653
654 Szilas, K., Hoffmann, J. E., Hansmeier, C., Hollis, J. A., Münker, C., Viehmann, S., & Kasper, H.
655 U. (2015a). Sm-Nd and Lu-Hf isotope and trace-element systematics of Mesoarchaean
656 amphibolites, inner Ameralik fjord, southern West Greenland. Mineralogical Magazine 79, 857-
657 876.
658
659 Szilas, K., Kelemen, P. B., & Rosing, M. T. (2015b). The petrogenesis of ultramafic rocks in the>
660 3.7 Ga Isua supracrustal belt, southern West Greenland: Geochemical evidence for two distinct
661 magmatic cumulate trends. Gondwana Research 28, 565-580.
662
663 Szilas, K., Tusch, J., Hoffmann, J.E., Garde, A.A., & Münker, C. (2016). Hafnium isotope
664 constraints on the origin of Mesoarchaean andesites in southern West Greenland, North Atlantic
665 craton. In: Archaean Cratons - New Insights on Old Rocks (Eds. J. Halla, M. Whitehouse, Z. Bagai,
666 T. Ahmad). Special Publication of the Geological Society of London (**in press**).
667
668 Vervoort, J. D., & Patchett, P. J. (1996). Behavior of hafnium and neodymium isotopes in the crust:
669 constraints from Precambrian crustally derived granites. Geochimica et Cosmochimica Acta,
670 60(19), 3717-3733.
671

672 Vervoort, J. D., Patchett, P. J., Söderlund, U., & Baker, M. (2004). Isotopic composition of Yb and
673 the determination of Lu concentrations and Lu/Hf ratios by isotope dilution using MC-ICPMS.
674 Geochemistry, Geophysics, Geosystems, 5(11).
675
676 Weyer, S., Münker, C., Rehkämper, M., & Mezger, K. (2002). Determination of ultra-low Nb, Ta,
677 Zr and Hf concentrations and the chondritic Zr/Hf and Nb/Ta ratios by isotope dilution analyses
678 with multiple collector ICP-MS. Chemical Geology, 187(3), 295-313.
679
680 Windley, B. F., & Garde, A. A. (2009). Arc-generated blocks with crustal sections in the North
681 Atlantic craton of West Greenland: crustal growth in the Archean with modern analogues. Earth-
682 Science Reviews, 93(1), 1-30.
683
684 **Figure captions**
685
686 Fig. 1. Geological map of the Nuuk region of southern West Greenland based on work by the
687 Geological Survey of Denmark and Greenland (GEUS). The Ivisaartoq Supracrustal Belt is located
688 in the eastern part of the map and the sampling area is outlined by a red box. The capital Nuuk is
689 marked with a red circle.
690
691 Fig. 2. Photomicrographs of the measured samples from the Ivisaartoq Supracrustal Belt. These
692 representative petrographic features are typical of amphibolite-facies metabasalts from this region.
693 a) Fine grained amphibolite (sample 499329) in plane polarized light (PPL). This rock is well-
694 foliated and is dominated by green hornblende and has less than 10 vol.% plagioclase and only
695 minor amounts of oxides. b) Sample 499329 under crossed polarized light (XPL). c) Medium grain
696 amphibolite (sample 499331) in PPL. d) Sample 499331 under XPL. e) Amphibole-bearing

serpentinite (sample 499321) in PPL. This sample is relatively oxide-rich, which likely represents magnetite formed after serpentinisation of olivine. f) Sample 499321 under XPL. Please note that the white scale bar at the lower right corner of each frame is 1 mm wide.

Fig. 3. Major element variation shown as a function of MgO content for various rocks from the Ivisaartoq Supracrustal Belt. Green circles represent mafic rocks, the large purple circle is the picritic rock and the red square is the serpentinite sample that were analysed as part of the present study. Small black dots are literature data for the volcanic sequence of the Ivisaartoq Supracrustal Belt extracted from the GeoRoc database (Sarbas & Nohl, 2008). Obvious alterations and metasedimentary rocks have been filtered out of the GeoRoc data set. Please note the cumulate trends that project towards olivine±opx (high-MgO) and cpx±amphibole (high-CaO) end-members, respectively. Also note that the sizes of the different symbols do not reflect the actual analytical uncertainties, which are significantly smaller.

Fig. 4. Primitive mantle-normalized trace element diagram for the new Ivisaartoq data presented in this study (green and purple lines). The outlier with the overall elevated trace element and positive Nb-anomaly is sample 499330, and sample 499331 has significantly lower Th content than the rest of the samples. Please note that the serpentinite sample (499321) is not shown due to its erratic pattern, as its trace element abundances are close to the detection limits, however even this sample is well within the total trace element range of the GeoRoc data for Ivisaartoq (not shown). The trace element composition of mean MORB (Gale et al., 2013) is shown for comparison (black diamonds).

Fig. 5. Pearce diagram for tectonic discrimination of volcanic rocks based on Th/Yb vs. Nb/Yb ratios. The data for the Ivisaartoq samples that were measured in the present study are given as large circles (green and purple) and the previously published data for the Ivisaartoq Supracrustal Belt

722 extracted from the GeoRoc database are shown as small black circles. Please note that displacement
723 from the mantle array is only possible by either crustal assimilation of by introduction of a
724 contaminant in the mantle source region. The latter is typically assumed to represent a slab-derived
725 component in the case of arc-related magmas (see inset in lower right corner). Also note that the
726 sizes of the different symbols do not reflect the actual analytical uncertainties, which is significantly
727 smaller.
728
729 Fig. 6. εHf_t versus time diagram showing the Hf-isotope data from the present study (large green
730 and purple circles) in comparison to literature data (small black circles). Southern West Greenland
731 samples denote Mesoarchaean basalts and andesites from the 2970 Ma Grædefjord supracrustal belt
732 (Szilas et al., 2013a), the 2970 Ma Fiskenæsset region (Szilas et al., 2012a), ca. 2970 Ma Ameralik
733 supracrustal belt (Szilas et al., 2015a), the ca. 2985 Ma Naajat Kuuat Anorthosite Complex
734 (Hoffmann et al., 2012), the >2996 Ma Tartoq Group (Szilas et al., 2011, 2013b), and the 3071 Ma
735 Qussuk Supracrustal Belt (Szilas et al., 2016). All of the data are for bulk-rock samples, except for
736 the Ivisaartoq data by Nutman et al. (2015c), which is based on in situ Hf-isotope analysis of zircon
737 extracted from a felsic volcanic rock (small blue diamonds). The isotope composition of the Isua
738 TTG is taken from Hoffmann et al. (2014) using their sample JEH 10–39 with a bulk-rock
739 $^{176}Lu/^{177}Hf$ ratio of 0.002351 and an εHf_{3806Ma} of +0.4±0.5.
740
741 Fig. 7. εHf_t vs. εNd_t diagram for the Ivisaartoq samples from the present study showing a deviation
742 from the mantle array (blue line). The picritic sample displays a significant displacement off the
743 mantle array, which we proposed could be due to TTG-restite entering the liquid at high enough
744 degree of melting of a heterogeneous mantle source. Please note that these data represent the only
745 samples from the Ivisaartoq Supracrustal Belt that have been analysed for both Lu-Hf and Sm-Nd

isotope compositions on the same rock. Also note that a similar range is observed for Archaean TTGs (not shown) according to Hoffmann et al. (2011b).

Fig. 8. Plots of Nb/Nb*, La/Sm and Th/Nb versus εNd_t and εHf_t, respectively. Please note that samples 499330 and 499331 have anomalous trace element patterns (see **Fig. 4**) with the former having a positive Nb-anomaly and the latter having low Th concentration relative to the rest of the samples. The picritic sample (499332), has a MgO contents of 12.2 wt.% and would have been expected to have the most depleted isotope composition of any of these rocks due to its higher degree of melting of the mantle source. However, we would argue that this is the reason why this particular sample may have entrained an unradiogenic Hf-component from TTG restite in the mantle source region (see discussion in the main text).

Tables

Table 1. Bulk-rock major and trace element data for the measured samples from the Ivisaartoq Supracrustal Belt. Please note that the ultramafic sample has an erratic trace element pattern, which suggests that this particular sample had incomplete digestion of accessory phases. For this reason we are only using the major element composition of this sample throughout this work.

Table 2. Bulk-rock Lu-Hf and Sm-Nd isotope data for the measured samples from the Ivisaartoq Supracrustal Belt. Please note that the ultramafic sample has an erratic trace element pattern (see **Table 1**), which suggests that this particular sample had incomplete digestion of accessory phases. This may explain why this sample has an unusually high apparent εHft compared to the rest of the samples. For this reason we are not using the isotope compositions of this particular sample in the discussion.

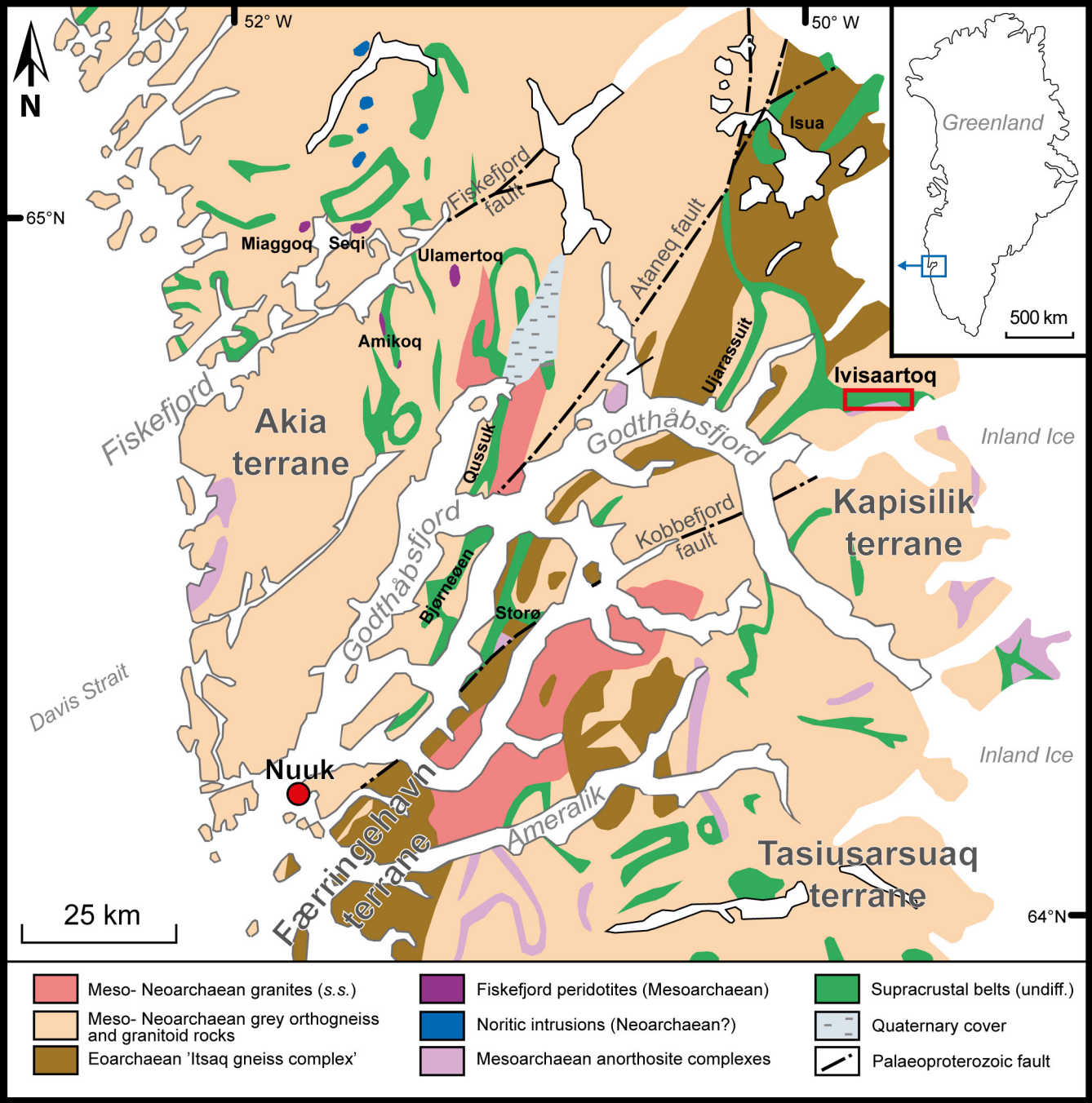
N
52° W
50° W
65°N
64°N
Greenland
500 km
Isua
Fiskefjord fault
Ataneq fault
Miaggoq
Seqi
Ulamertoq
Amikoq
Ujarassuit
Ivisaartoq
Fiskefjord
Akia terrane
Qussuk
Godthåbsfjord
Inland Ice
Kapisilik terrane
Kobbefjord fault
Bjørnegaen
Storø
Godthåbsfjord
Davis Strait
Nuuk
Ameralik
Færingehavn terrane
Tasiusarsuaq terrane
Inland Ice
25 km
Meso- Neoarchaean granites (s.s.)
Meso- Neoarchaean grey orthogneiss and granitoid rocks
Eoarchaean 'Itsaq gneiss complex'
Fiskefjord peridotites (Mesoarchaean)
Noritic intrusions (Neoarchaean?)
Mesoarchaean anorthosite complexes
Supracrustal belts (undiff.)
Quaternary cover
Palaeoproterozoic fault

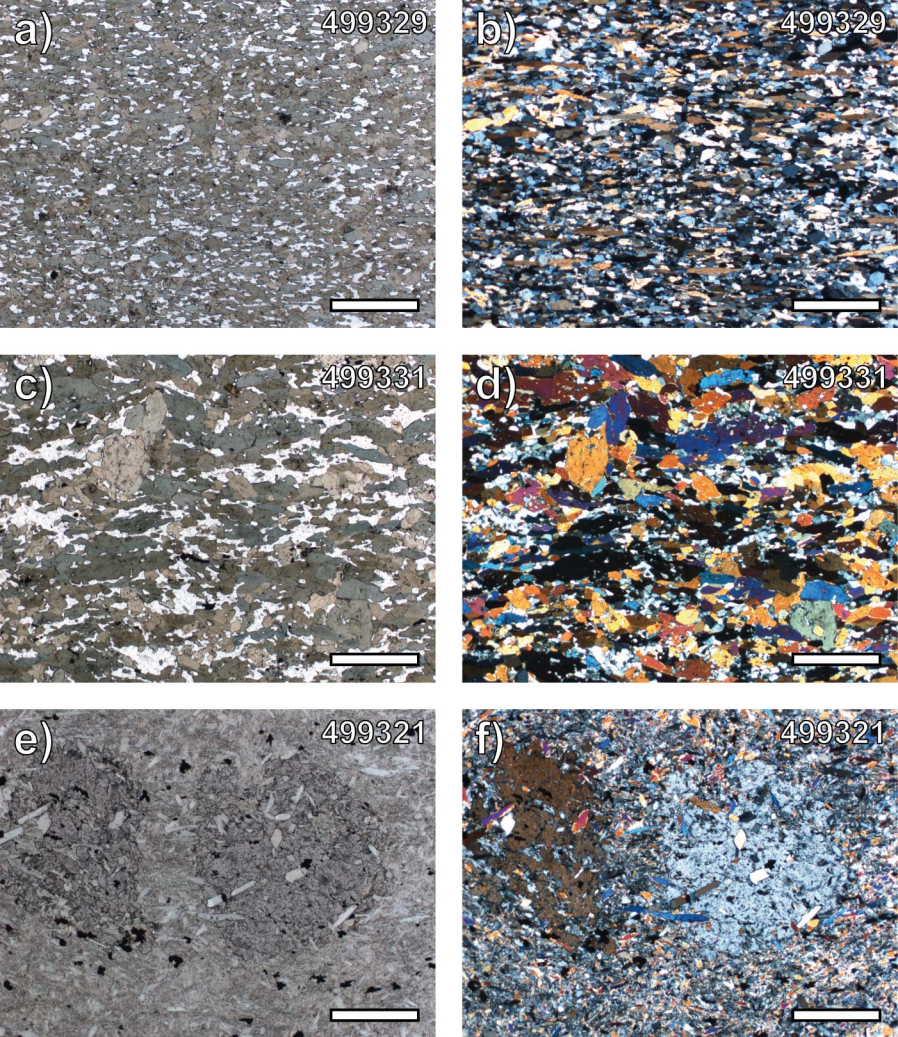
a)
499329
b)
499329
c)
499331
d)
499331
e)
499321
f)
499321

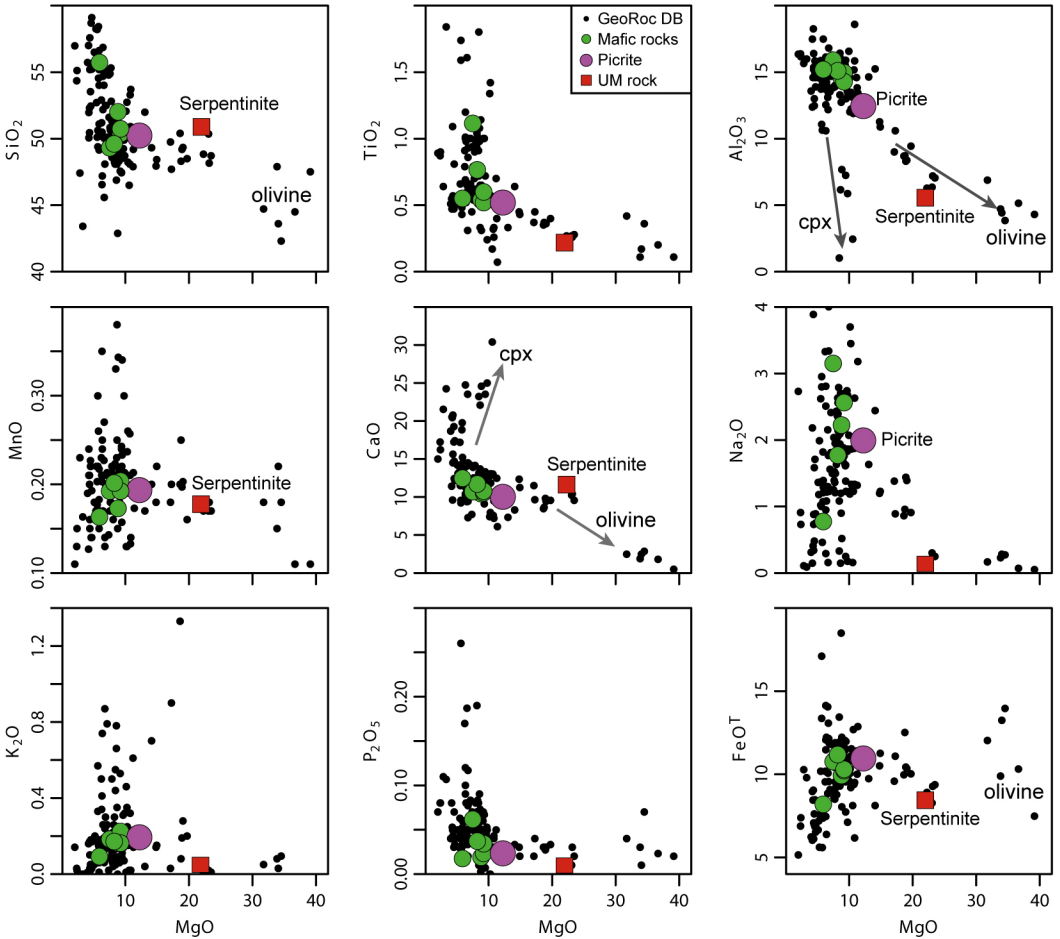
GeoRoc DB
Mafic rocks
Picrite
UM rock
SiO2
TiO2
Al2O3
MnO
CaO
Na2O
K2O
P2O5
FeOT
MgO
Serpentinite
olivine
Picrite
cpx

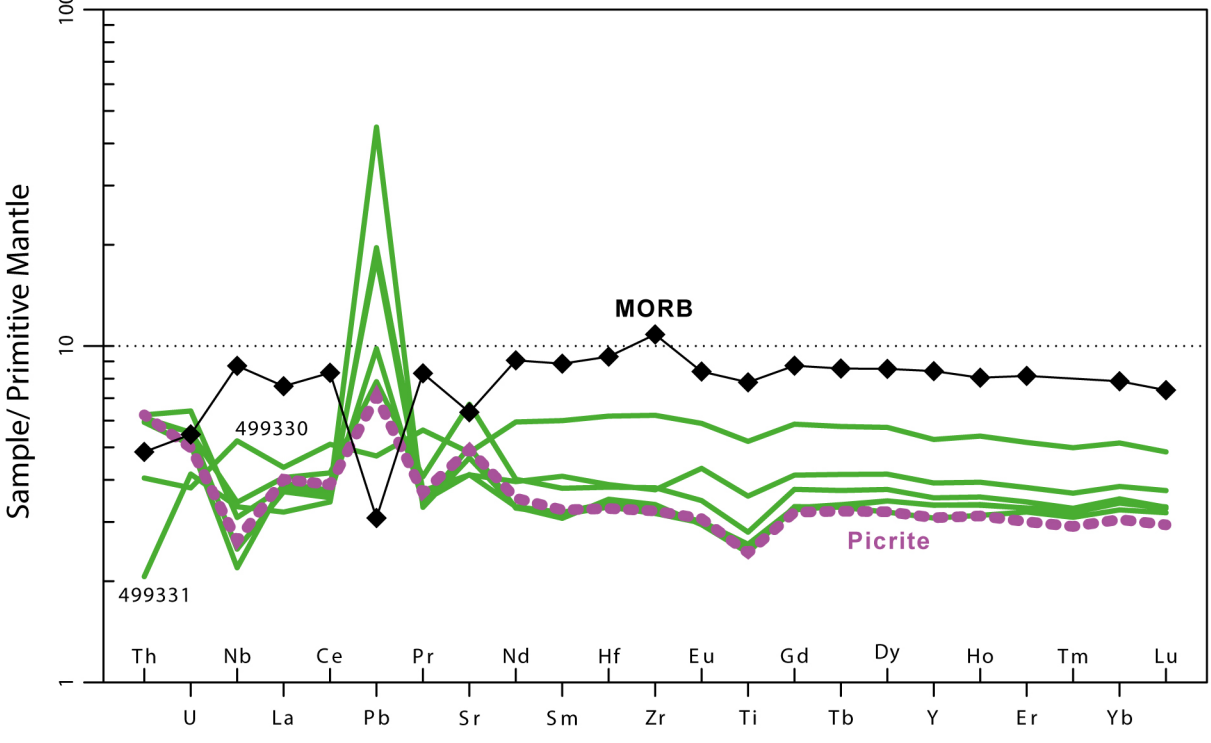
Sample/ Primitive Mantle
100
10
1
MORB
499330
499331
Picrite
Th
Nb
Ce
Pr
Nd
Hf
Eu
Gd
Dy
Ho
Tm
Lu
U
La
Pb
Sr
Sm
Zr
Ti
Tb
Y
Er
Yb

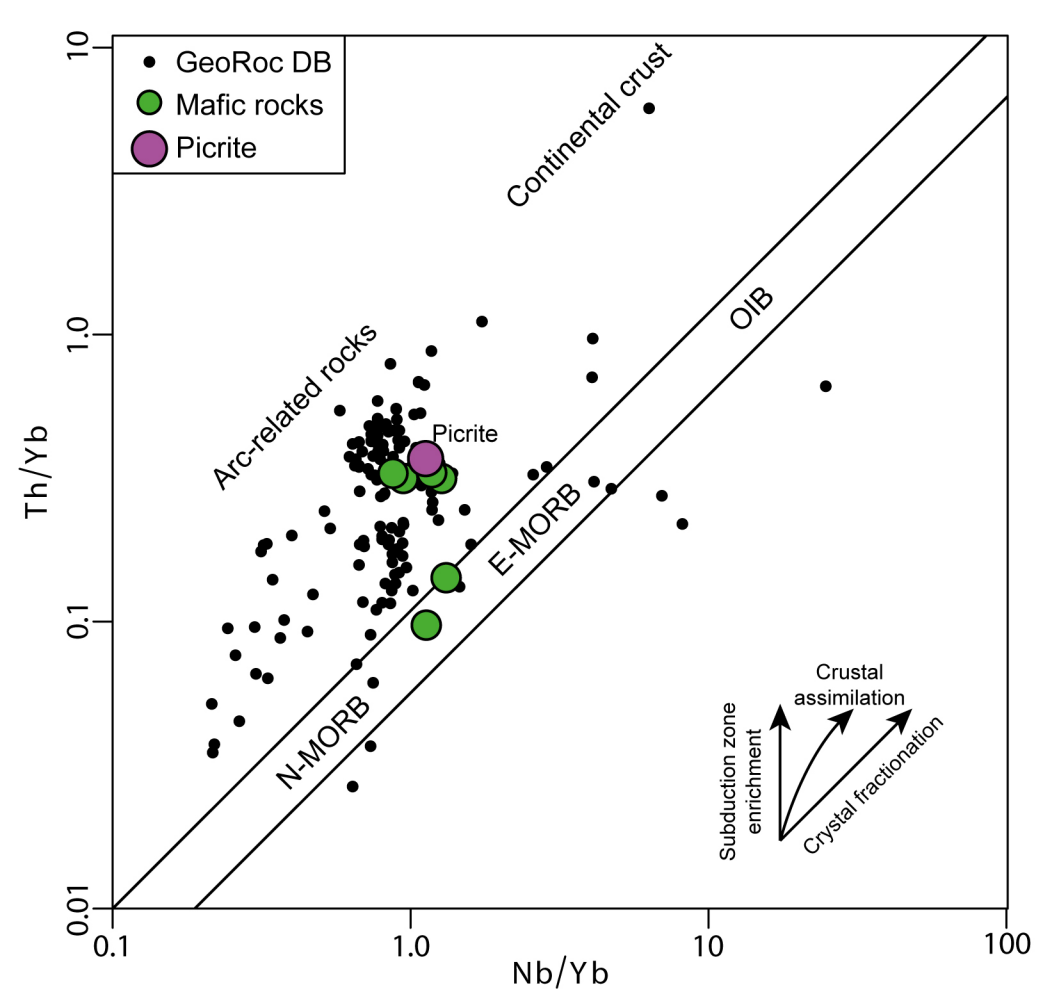
GeoRoc DB
Mafic rocks
Picrite
Continental crust
OIB
E-MORB
N-MORB
Arc-related rocks
Picrite
Crustal assimilation
Subduction zone enrichment
Crystal fractionation
Th/Yb
Nb/Yb
10
1.0
0.1
0.01
0.1
1.0
10
100

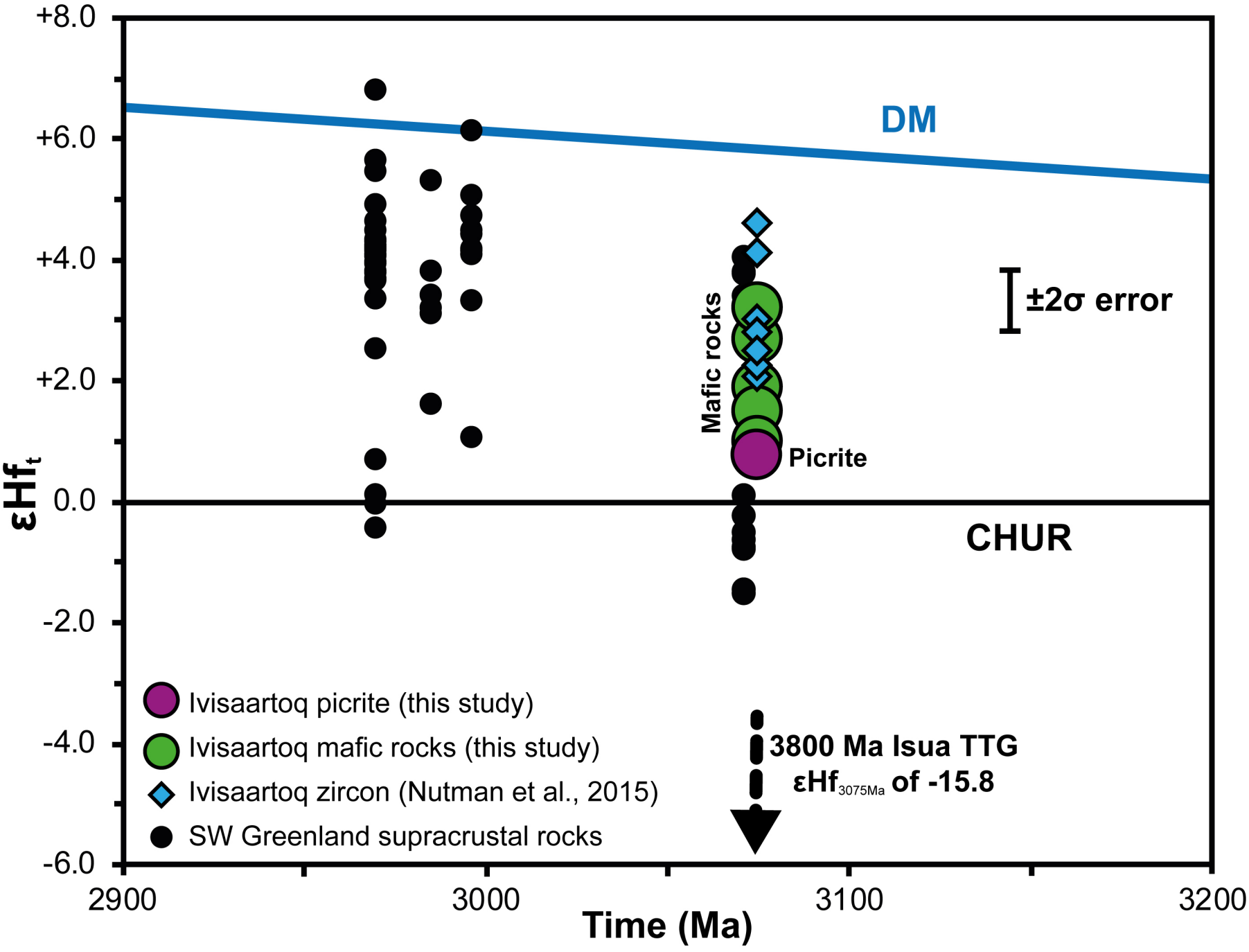
+8.0
+6.0
+4.0
+2.0
0.0
-2.0
-4.0
-6.0
εHf$_t$
DM
CHUR
±2σ error
Mafic rocks
Picrite
Ivisaartoq picrite (this study)
Ivisaartoq mafic rocks (this study)
Ivisaartoq zircon (Nutman et al., 2015)
SW Greenland supracrustal rocks
3800 Ma Isua TTG
εHf$_{3075Ma}$ of -15.8
2900
3000
3100
3200
Time (Ma)

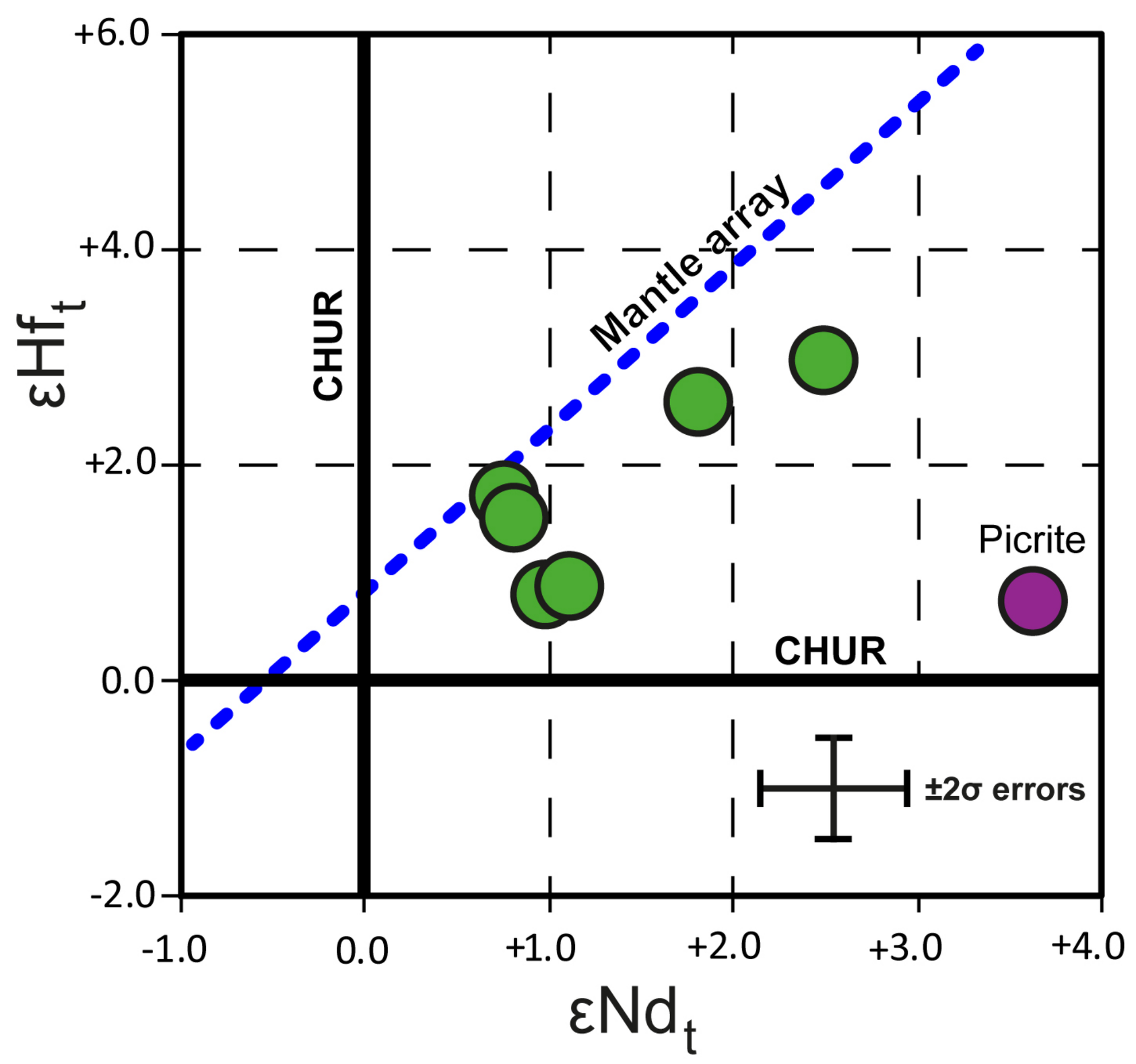
+6.0
+4.0
+2.0
0.0
-2.0
εHf$_t$
CHUR
Mantle array
Picrite
CHUR
±2σ errors
-1.0
0.0
+1.0
+2.0
+3.0
+4.0
εNd$_t$

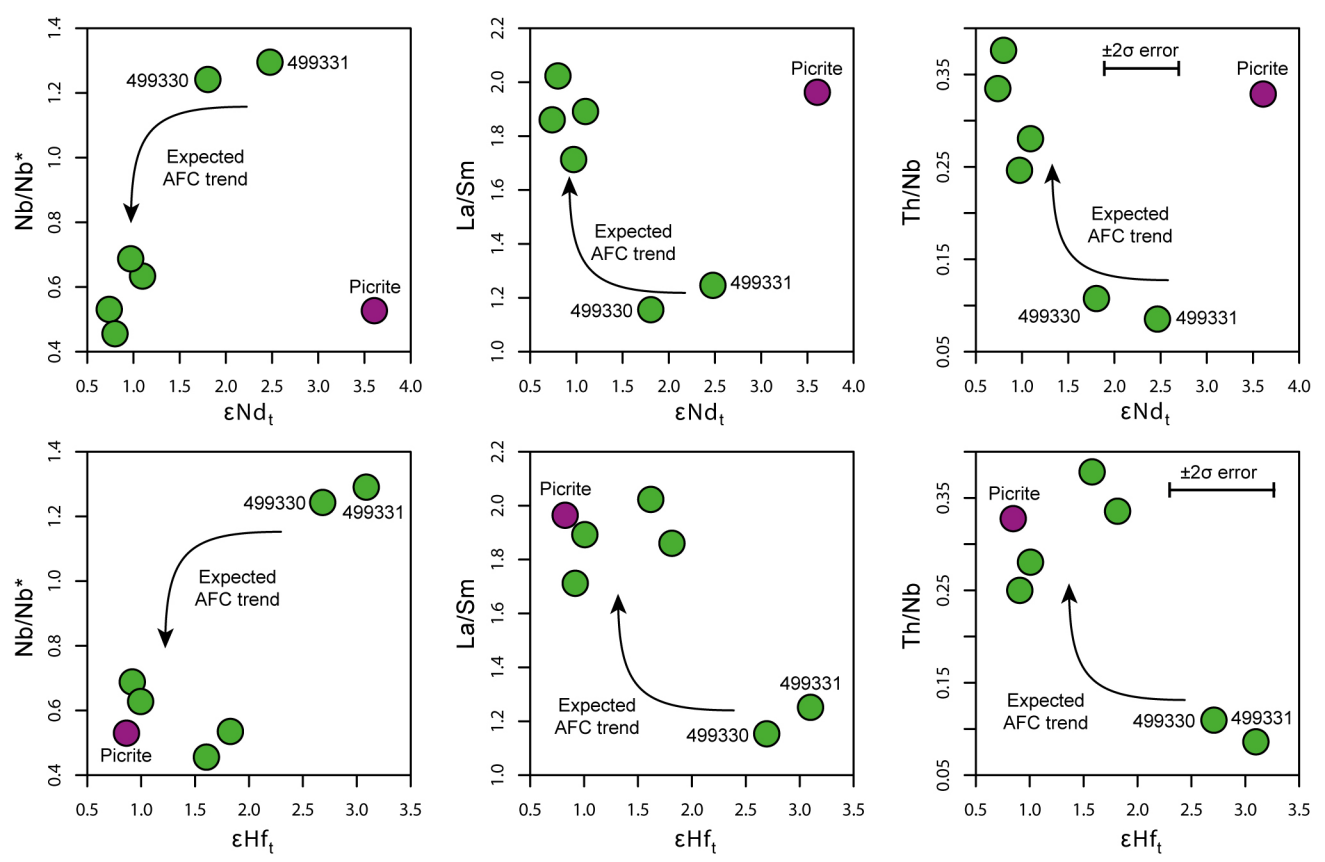
Nb/Nb*
εNd$_t$
499330
499331
Expected
AFC trend
Picrite
La/Sm
εNd$_t$
Picrite
Expected
AFC trend
499330
499331
Th/Nb
εNd$_t$
±2σ error
Picrite
Expected
AFC trend
499330
499331
Nb/Nb*
εHf$_t$
499330
499331
Expected
AFC trend
Picrite
La/Sm
εHf$_t$
Picrite
499331
Expected
AFC trend
499330
Th/Nb
εHf$_t$
±2σ error
Picrite
Expected
AFC trend
499330
499331

Sample	499321	499325	499327	499328	499329	499330	499331	499332
Rock type	Ultramafic rock	Amphibolite	Pillow core	Metagabbro	Pillow lava	Amphibolite	Pillow lava	Picrite
Latitude	N 64°43.690	N 64°44.768	N 64°44.830	N 64°44.899	N 64°44.899	N 64°44.809	N 64°44.538	N 64°44.381
Longitude	W 49°54.523	W 49°51.336	W 49°52.324	W 49°51.845	W 49°51.845	W 49°51.522	W 49°57.660	W 49°56.182
Majors (wt.%)								
SiO2	48.83	51.20	54.67	49.48	50.05	48.71	49.27	49.34
TiO2	0.21	0.53	0.54	0.51	0.59	1.10	0.76	0.51
Al2O3	5.26	14.32	14.89	14.68	14.07	15.70	14.98	12.23
Fe2O3	9.01	10.86	8.93	11.15	11.27	11.80	12.34	11.94
MgO	21.08	8.69	5.82	9.04	9.09	7.40	8.16	12.00
MnO	0.17	0.17	0.16	0.20	0.19	0.19	0.20	0.19
CaO	11.20	10.27	12.21	10.38	10.65	10.54	11.61	9.83
Na2O	0.13	2.19	0.76	2.52	2.53	3.11	1.76	1.96
K2O	0.03	0.16	0.09	0.22	0.16	0.18	0.17	0.19
P2O5	0.01	0.02	0.02	0.02	0.03	0.06	0.04	0.02
SO3	0.03	0.01	0.06	0.01	0.01	0.01	0.03	0.01
LOI	3.35	0.73	0.43	0.72	0.52	0.54	0.58	0.93
Total	99.6	99.3	98.7	99.0	99.3	99.5	100.0	99.3
Traces (ppm)								
Li	-	53.7	35.8	-	77.0	85.6	167	119
Sc	-	44.5	45.4	41.9	38.9	46.9	42.4	39.4
V	-	250	254	-	237	321	273	225
Cr	-	429	779	385	491	291	312	909
Co	-	47.8	67.7	-	53.2	50.8	52.0	63.4
Ni	-	120	318	118	138	119	158	326
Cu	-	17.8	69.0	28.2	49.1	24.9	106	80.4
Zn	-	71.8	88.7	80.0	82.3	101	88.2	84.5
Ga	-	14.4	14.1	-	14.4	18.7	16.1	12.8
Rb	-	1.18	1.03	17.7	1.69	5.63	3.04	5.64
Sr	26.7	102	84.2	94.4	136	97.9	84.1	100
Y	6.84	14.7	14.7	13.5	15.5	23.1	17.1	13.5
Zr	12.7	34.3	35.2	36.5	40.9	67.2	40.4	34.9
Nb	0.80	1.49	1.86	1.32	2.06	3.13	2.00	1.58
Mo	-	0.219	0.587	-	0.0685	0.132	0.106	0.113
Sn	-	0.324	0.445	-	0.421	0.656	0.432	0.362

Sb	-	0.109	0.132	-	0.239	0.134	0.126	0.395
Cs	-	0.0411	0.0186	1.57	0.00266	1.16	0.0592	0.447
Ba	-	50.7	25.2	41.9	46.4	50.7	25.0	43.6
La	2.40	2.53	2.61	2.68	2.79	2.99	2.20	2.76
Ce	5.51	6.32	6.49	6.64	7.49	9.11	6.14	6.91
Pr	-	0.911	0.933	0.895	1.104	1.519	1.003	0.989
Nd	3.40	4.38	4.42	4.40	5.33	7.89	5.25	4.68
Sm	1.13	1.36	1.38	1.33	1.63	2.59	1.77	1.40
Eu	0.347	0.483	0.487	0.477	0.562	0.954	0.701	0.497
Gd	1.72	1.86	1.89	1.90	2.14	3.34	2.36	1.83
Tb	0.285	0.351	0.354	0.35	0.391	0.605	0.436	0.339
Dy	-	2.46	2.46	2.28	2.66	4.07	2.96	2.29
Ho	0.469	0.535	0.537	0.499	0.566	0.858	0.626	0.497
Er	1.50	1.54	1.53	1.49	1.60	2.40	1.77	1.40
Tm	-	0.234	0.230	0.223	0.237	0.359	0.263	0.209
Yb	1.638	1.579	1.576	1.505	1.622	2.379	1.767	1.409
Lu	0.136	0.238	0.236	0.229	0.238	0.347	0.267	0.211
Hf	0.560	0.997	1.03	1.05	1.14	1.86	1.16	0.986
W	0.0376	0.225	0.505	-	0.206	0.168	0.288	0.153
Tl	-	0.00489	0.00207	-	0.00860	0.0306	0.0439	0.0300
Pb	-	3.40	1.82	8.28	1.45	0.87	3.63	1.31
Th	-	0.498	0.521	0.495	0.510	0.338	0.172	0.520
U	0.419	0.121	0.140	0.111	0.121	0.0825	0.0907	0.109

	Lithology	Lu (ppm)	Hf (ppm)	Lu/Hf	$^{176}Lu/^{177}Hf$	2σ error	$^{176}Hf/^{177}Hf$	2σ error	εHf_{3075Ma}	2σ error
499321	Ultramafic rock	0.1382	0.6417	0.2154	0.03058	0.00007	0.282816	0.000009	7.5	0.5
499325	Amphibolite	0.2469	1.047	0.2357	0.03346	0.00008	0.282827	0.000006	1.8	0.5
499327	Pillow core	0.2464	1.072	0.2298	0.03262	0.00007	0.282756	0.000008	1.0	0.5
499328	Metagabbro	0.2333	1.009	0.2313	0.03283	0.00008	0.282785	0.000006	1.6	0.5
499329	Pillow lava	0.2469	1.201	0.2056	0.02918	0.00008	0.282549	0.000005	0.9	0.5
499330	Amphibolite	0.3605	1.907	0.1890	0.02683	0.00006	0.282460	0.000005	2.7	0.5
499331	Pillow lava	0.2722	1.186	0.2295	0.03258	0.00008	0.282810	0.000011	3.1	0.8
499332	Picrite	0.2191	1.038	0.2111	0.02996	0.00016	0.282594	0.000005	0.8	0.5